

# On the Joint Design and Hydraulic Actuation of Octahedron VGT Robot Manipulators

Sven Rost, Matthias Uhlemann, Karl-Heinz Modler, Yevgen Sklyarenko,  
Frank Schreiber and Walter Schumacher

**Abstract**—In this paper, the design for variable geometry truss manipulators, with 3-DOF octahedron-shaped modules and hydraulic actuation is introduced. The main features of the concept are the optimized multiple collocated spherical joints and a structure-integrated supply of the drive fluid for the hydraulic actuators. Based upon the known Spherical Joint Mechanism, design rules are deduced and modified joint elements are presented to provide a larger workspace for a single module. The potential of the resulting module design is demonstrated by the calculation of the workspace, as well as the payload-to-mass ratio. Based upon the presented results, a family of highly maneuverable light-weight hyper-redundant manipulators can be derived.

## I. INTRODUCTION

Hyper-redundant robots represent a subclass of the redundant robots and have a high degree of kinematic redundancy [1]. This class of robots has attracted a lot of attention, because these robots can be used to manipulate in an environment with many obstacles, to handle objects with the whole manipulator structure instead of using specific tools and for new kinds of locomotion, e.g. snake-like crawling [2]. Kinematically redundant manipulators usually possess a larger dextrous workspace, than their non-redundant counterparts, due to the possibility to avoid of joint limitations and singular configurations of the manipulator, as well as obstacles within the workspace.

Our research is focused on the development of a robot design, which allows the construction of kinematically hyper-redundant manipulators with the following characteristics:

- light-weight mechanical structure, resulting in low energy consumption, high payload-to-weight ratio and highly dynamic motion through low mechanical inertia;
- high stiffness-to-weight ratio, resulting in precise control of the manipulator, as well as good handling characteristics;
- low energy consumption during static holding operation;
- composition of identical modules containing one translational and two rotatory degrees of freedom (DOF), resulting in easy scalability of the manipulator and low complexity of kinematics and actuation.

Manuscript received on 08.02.2011.

Sven Rost is with the National Technical University Donetsk, Department of Control Systems and Mechatronics, Artema 58, 83000 Donetsk, Ukraine.

Matthias Uhlemann and Karl-Heinz Modler are with the Dresden University of Technology, Institute of Solid Mechanics, 01062 Dresden, Germany.

Yevgen Sklyarenko, Frank Schreiber and Walter Schumacher are with the Technical University Braunschweig, Institute of Control Engineering, Hans-Sommer-Str. 66, 38106 Braunschweig, Germany.

Corresponding author: post@sven-rost.de

## II. CONCEPT FOR A HYDRAULICALLY DRIVEN MODULAR MANIPULATOR DESIGN

### A. Selection of the kinematic structure

The class of hyper-redundant robots can be divided into three main groups [3]: highly segmented serial robots, hybrid serial-parallel robots and continuous robots. Because of their inherent underactuation and the resulting problems in modeling and control, the group of continuous robots was disconsidered from our study. Accordingly, we chose kinematic structures from the groups of segmented serial and hybrid serial-parallel robots, which allow an actuation with gear-less long-stroke linear actuators, while fulfilling the required number and types of DOF's. In a second step we compared the selection of kinematic structures shown in Fig. 1. Along with the necessary aspects from the introduction, the following criteria were considered using a weighted value benefit analysis:

- low bending moments on actuators and links;
- minimum number of actuators for the claimed DOF's;
- reduced complexity of joint construction;
- large dextrous workspace of the composed manipulator.

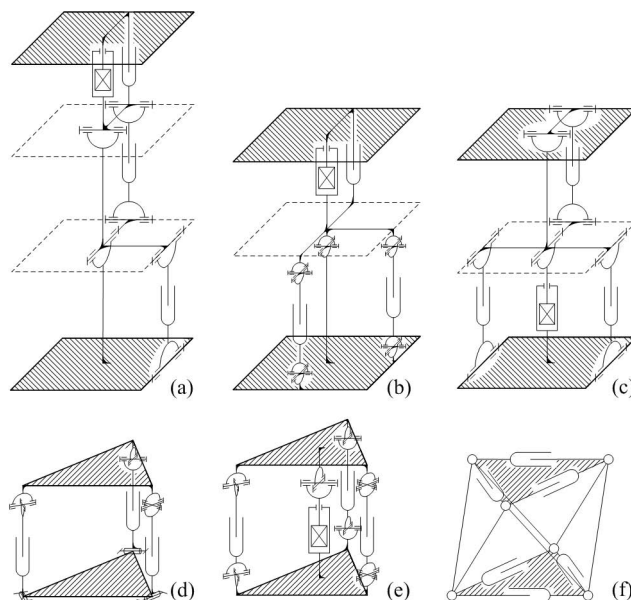


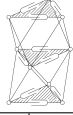

Fig. 1. Compared kinematic structures: serial modules (a), hybrid modules with Cardan joint (b) and with translational-rotatory joint (c), parallel modules with cylinders subjected to bending forces (d) and with a passively hinged connection (e), octahedron-shaped VGT-module (f).

The best results were achieved with kinematic concepts based on a variable geometry truss (VGT), see Fig. 1(f). VGT-concepts are already well known since the 80's, and they were mainly shaped in tetrahedron [4] and in octahedron geometry [5], [6], [7]. Of all the VGT geometries, only the octahedron geometry achieves the necessary number of DOF per module and favorable dynamic properties [6], [7].

### B. Choice of the actuation technology

For the chosen octahedron-shaped VGT two actuation concepts are of interest: either the actuation of every horizontal triangle of the structure [5] or to actuate every second horizontal triangle in the structure [7]. The length of the passive links of the vertical triangles, and the minimum and maximum length of the active links in the horizontal triangles are directly determining the workspace of a module and consequently the workspace of the manipulator. We compared the actuation principles with respect to the resulting size of the workspace and the maneuverability of the composed structure. To visualize the results, the ability to fold and bend as a function of the length ratio  $k$  and the type of actuation is depicted in Tab. I for a structure composed of four modules (passive link lengths are chosen equal to the minimal active link lengths). A concept with actuation of every horizontal triangle and a high maximum-minimum-length ratio  $k$  of the active links was chosen, resulting in a larger usable workspace, which is indicated by a higher folding and bending capability of the structure.

TABLE I  
FOLDABILITY AND STRUCTURAL CURVATURE DEPENDING OF THE  
ACTUATION PRINCIPLES AND THE LENGTH RATIO  $k$

|            |  |      |  |     |
|------------|---|------|---|-----|
| $k = 1, 3$ | 85%   | 56°  | 89%   | 39° |
| $k = 1, 4$ | 78%   | 81°  | 85%   | 56° |
| $k = 1, 5$ | 70%   | 111° | 79%   | 76° |
| $k = 1, 6$ | 59%   | 157° | 72%   | 99° |

Linear actuators are the least complex way to drive the VGT structure. Moreover conventional drive technologies like electric, hydraulic or pneumatic drives can be applied here, while other technologies, like e.g. shape memory alloys, electro-active polymers or piezoelectric actuators will not provide the required relationship between attainable force and permissible stroke without the use of gears. In order to achieve a high payload-to-mass ratio of the structure, the actuators have to provide a high force-to-mass ratio.

While in the beginning of the robot-technology hydraulic drives were the state of the art in actuation [8], [9], at the moment they are not very common in robot structures. Some historic technical problems resulted in the wide-spread substitution with electric drives, which were developed faster and allowed easier integration and control [8], [10]. The main disadvantages of hydraulic systems were their difficult controllability, leakage, expensive and complex components for power supply and controlling [8], [10], [2]. Nowadays these disadvantages are nearly completely eliminated, which makes hydraulic actuation interesting again for a use in robotics. Hydraulic drives can reach a very high power-to-mass ratio, inherent through their working principle, as well as high forces due to high pressure levels of the fluid and the reduction of moved masses by the separation of power supply and actuating part [14]. Because of these facts and other advantageous characteristics, like:

- high forces and low mechanical inertia through direct linear movement without the need of mechanical gear, resulting in a high dynamics,
- simple construction of linear actuators, resulting in robust design,
- high stiffness in comparison to pneumatic drives, allowing precise position control,
- nearly zero energy consumption of valve-controlled actuators in halted state,

hydraulic drives were chosen as the means of actuation for the presented VGT modules.

The feasibility of hydraulic actuation for redundant manipulators has been proven by a few successful redundant robot designs, most notably the Schilling Titan 4 [11] and SARCOS Dextrous Arm [12], both with seven DOF's and Zhao's ten DOF robot arm [13].

### C. Design of the hydraulic power supply routing

To realize the drive fluid supply to the actuators, a variety of solutions under usage of hydraulic hoses and pipes is imaginable. Three approaches are depicted in Fig. 2. In the left realization, one main hose is used for pressure supply and the other main hose for tank connection. Both pass through the whole structure and are connected with each module through a separator to split the hoses at each segment. The advantage of this variant is its simple setup. The disadvantage is the necessity for long and unrestrainedly moving hoses, which can result in pinching of the hoses between structure elements. In Fig. 2 (middle) there are three main power and tank hoses going through the whole structure (for reason of clarity just one pair is depicted). The hoses are routed

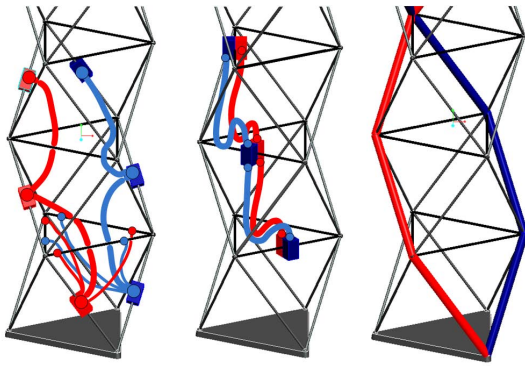


Fig. 2. Possible realizations for the fluid supply through the structure.

pairwise (pressure and tank) and directly connect the power ports of one actuator per module. The hoses only have to transport one third of the maximum flow and can be designed shorter and with smaller diameter - which increases the hydraulic stiffness and decreases the danger of pinching between structure elements. In Fig. 2 (right) the passive links of the structure are designed as hydraulic pipes to transport the fluid. Due to the fact, that there are six passive links in each module, it is - like in the previous solution - possible to use three links for power and three links for tank supply. On each link a branch is implemented from which the power supply port of the respective actuator is connected with a conventional hydraulic hose. Also the ends of the passive links are connected with hydraulic hoses - due to the fact that these hoses have to cross each other in each joint point of the structure, special attention has to be paid to the routing of the hoses in the joints.

This last variant is selected due to the advantage, that there are no separate and unrestrainedly moving hydraulic hoses within the structure. In addition, the resulting system possesses a high hydraulic stiffness because of its rigid hydraulic pipes and minimal hose length (reduced up to 80 percent in comparison to the other presented variants).

#### D. Analysis and design of the joints

In order to avoid bending moments on the links, which would decrease the maximum load capacity of the structure, the goal was to use spherical joints - in contrast to the quasi spherical joint originally introduced by Miura for the VGT structure, see Fig. 3 (left). An interesting principle to realize spherical joints was published by Hamlin and Sanderson with the CMS joint [16], see Fig. 3 (middle). A collection of many other principles of multiple collocated joints is presented in [17], and the author recommends the use of a so called Spherical Joint Mechanism (SJM) see Fig. 3 (right). These two joints, CMS and SJM, allow the design of rigid multicollated spherical joints necessary for the structure.

As we want to use the passive links of the structure as hydraulic pipes, the joints have to provide enough space between the endings of the passive links in order to connect them with hydraulic hoses. Here a disadvantage of the CMS joint appears: the fixing points for the joint kinematic on

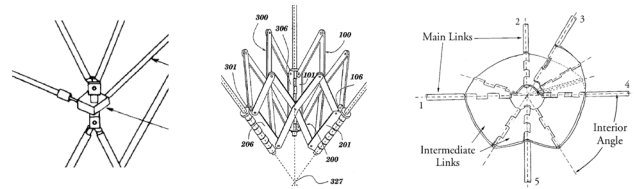


Fig. 3. Quasi spherical consecutive joint proposed by Miura [5] (left), CMS joint by Hamlin (middle) and SJM joint by Bosscher [17] (right).

two connecting links have to have the same geometrical arrangement. In order to have sufficient space between the ends of passive links, the bearings of the passive links have to be further away from the joints virtual center of rotation. Due to the necessary symmetry of the CMS joint, the fixing points of the active links would also have to have the same distance to the virtual rotation point. This would decrease the length ratio  $k$  of the active links close to one, meaning that the structure would be nearly unmovable. In contrast, the SJM joint can be designed unsymmetrically - the passive links can be located distant from the virtual rotation point to provide space for the attachment of hoses, and those of the active links can be positioned close to the virtual rotation point, to reduce dead length, providing a high length ratio  $k$ .

We evaluated the SJM and CSM joints under constructive, mechanical and kinematic aspects for the octahedron VGT structure. For the constructive dimensioning of the joint, we used a static force model (see Chapter III-B), which included the masses of the structural components, as well as the maximal permissible actuator forces. These configurations were determined in which the maximal force loads act upon the joints. This allowed to calculate the material stress and deformation distribution within the joints. Under similar loading conditions and optimized design of both joints, the CMS suffers from significantly larger deformations, see Fig. 4. Additionally, due to its construction the CMS design is subjected to up to 3-times higher material stress, mainly in areas in which hardly reducible notch-stress exists (arrow in Fig. 4).

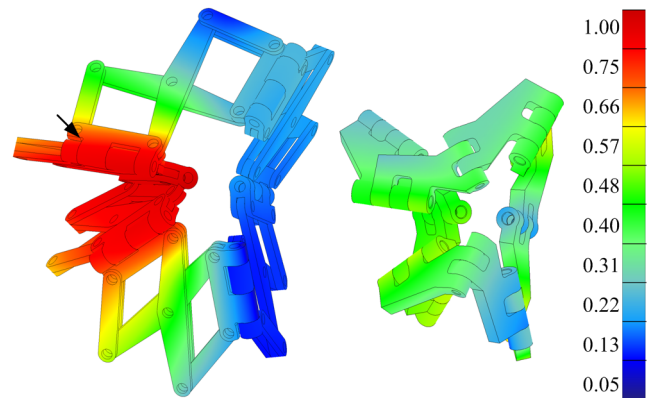


Fig. 4. Deformation distribution in a maximum load configuration for CMS joint (left) and SJM joint (right), normalized by peak values in CMS joint.

In direct comparison of the two joints, which we researched on a variant of VGT with external power supply, the CMS joint also had other unfavorable characteristics like, a 38 percent larger mass, 36 percent lower stiffness, 20 percent longer joints (increasing the links' dead length) as well as a lower minimum angle because of complex inner kinematic. Therefore, the SJM was selected for the module and its design was adjusted according to the criteria presented in the next section.

### E. Modification of the joints

Beginning from a basic model close to the original design [16], [17] (see Fig. 5) the specific construction of the joint was done in an iterative process in which we sought an optimum between rigidity, joint mass, movability/collision, load capacity and the length of the joints in order to achieve a high length ratio  $k$ , a large number of similar parts and a reduced construction complexity.

In order to avoid singularities and to ensure that the joints turn into the designed directions, the maximal opening angle  $\alpha_{max}$  must be smaller than the maximum angle of the joint ( $\alpha_1 + \alpha_2$ ). A central problem for the usage of the SJM joint in the octahedron VGT structure is collision avoidance: there are two types of collisions existing, the outer (joint-to-joint) and the inner (plate-to-plate) collision, see Fig. 6.

To avoid the outer collision between two neighboring joints in one joint knot, see Fig. 6 (left) and (middle), we found three design rules:

- 1) Minimization of the maximum opening angle of the joint close to the maximum opening angle of the connected links. This rule results in two differently sized joint types in one knot, because the maximum opening angle of the passive links is larger than the opening angle between the passive and the active links.
- 2) The joints between the passive links have to swivel out of the octahedron and the joints between one passive and one active link have to turn into the octahedron.
- 3) Movement of the inner joint bearings has to be directed away from and the movement of the outer joint bearings into the direction of the instantaneous center of rotation respectively.

To avoid an inner collision of a whole joint, see Fig. 6 (right), we determined two design rules:

- 1) To avoid collision of the plates connected pairwise to one main link, the plates have to move sideways, away from the center of rotation.
- 2) The bearing-bridges are spared.

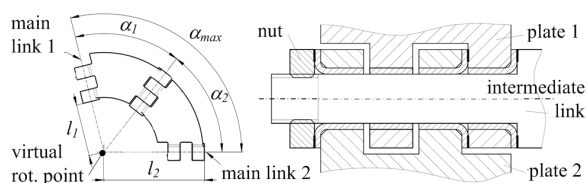


Fig. 5. Basic joint model based upon the original SJM design (left) by Bosscher [17], bearing design of the SJM joint rotation axes (right).

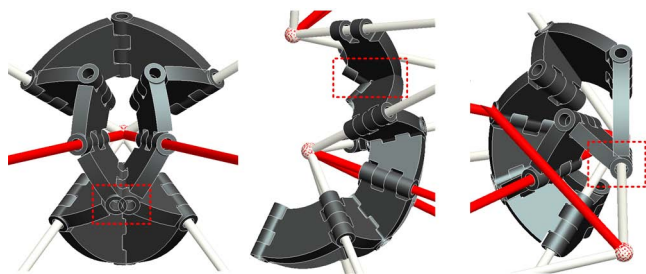


Fig. 6. Collision scenarios of the plate joint (SJM): inner collision within a joint (left), outer plate joints (middle) and outer collision between two neighboring joints (right).

To allow enough space between the ends of the passive links to connect them with the hydraulic hoses (hose length plus two times the length of the adapter), the fixture of these passive links has to be located at a distance to the virtual rotation center. This distance is limited because it increases the joint weight and the decreases the stiffness of the joint. The same problem is caused by increasing the diameter of the passive link - so there is also a trade-off between the loss of hydraulic energy, mainly influenced by the diameter of passive link, and the mass and stiffness of the joint.

In order to avoid collisions, and to retain sufficient space to connect the passive links with hydraulic hoses, the spherical joint plates were redesigned in a trapezoid shape. This construction has two different types of plate joints, as depicted in Fig. 9 - ingoing joints to connect the actuators with passive links, and outgoing joints to connect the passive links with each other. The outgoing joints are thicker than the plate joints connecting active and passive links, because they are longer and so the danger of buckling is higher.

## III. KINEMATIC ANALYSIS OF A MODULE

To evaluate the designed modules, a workspace and stiffness analysis will be performed for a single module. The following subsection will present a method to solve the direct kinematics based upon vector geometry and optimization to derive the modules' workspace. Consequently, a method to compute the forces within the structure is introduced to derive the stiffness model.

### A. Direct kinematics and workspace analysis

The direct kinematics can be solved successively from the base to the top module with the knowledge of the basis' joint-points  $\mathbf{A}_0, \mathbf{B}_0, \mathbf{C}_0$  defined in the base coordinate system  $x_0, y_0, z_0$ , the length of the passive links  $l_p$  and the three active link lengths  $L_{i,1}, L_{i,2}, L_{i,3}$  of each module  $i$ . We can define all vectors in Fig. 7 with the following algorithms.

- 1) The joint-points  $\mathbf{A}_i, \mathbf{B}_i$  and  $\mathbf{C}_i$ , which represent the basis' joint-points for  $i = 0$  or the following joint-points derived in the iteration steps for  $i > 0$ , span a plane with the normal unit vector:

$$\mathbf{n}_i = \frac{\mathbf{A}_i \times \mathbf{B}_i + \mathbf{B}_i \times \mathbf{C}_i + \mathbf{C}_i \times \mathbf{A}_i}{\|\mathbf{A}_i \times \mathbf{B}_i + \mathbf{B}_i \times \mathbf{C}_i + \mathbf{C}_i \times \mathbf{A}_i\|} \quad (1)$$

- 2) With the normal vector  $\mathbf{n}_i$  and the direction vectors of the active links, the unit vectors  $\mathbf{t}_{i,1...3}$  can be computed, which are lying in the perpendicular bisector of the base triangle sides and are orientated out of the spanned plane:

$$\mathbf{t}_{i,1} = \frac{(\mathbf{B}_i - \mathbf{A}_i) \times \mathbf{n}_i}{\|(\mathbf{B}_i - \mathbf{A}_i) \times \mathbf{n}_i\|} \quad (2)$$

$$\mathbf{t}_{i,2} = \frac{(\mathbf{C}_i - \mathbf{B}_i) \times \mathbf{n}_i}{\|(\mathbf{C}_i - \mathbf{B}_i) \times \mathbf{n}_i\|} \quad (3)$$

$$\mathbf{t}_{i,3} = \frac{(\mathbf{A}_i - \mathbf{C}_i) \times \mathbf{n}_i}{\|(\mathbf{A}_i - \mathbf{C}_i) \times \mathbf{n}_i\|} \quad (4)$$

- 3) Then the heights of each side triangle, formed by one active and two passive links, are computed:

$$h_{i,1} = \sqrt{l_p^2 - (1/2 \cdot \|\mathbf{B}_i - \mathbf{A}_i\|)^2} \quad (5)$$

$$h_{i,2} = \sqrt{l_p^2 - (1/2 \cdot \|\mathbf{C}_i - \mathbf{B}_i\|)^2} \quad (6)$$

$$h_{i,3} = \sqrt{l_p^2 - (1/2 \cdot \|\mathbf{A}_i - \mathbf{C}_i\|)^2} \quad (7)$$

- 4) In the next step the joint points of the following plane are computed in dependence of the angles  $\phi_{i,1...3}$ :

$$\mathbf{A}_{i+1} = (\mathbf{B}_i + \mathbf{C}_i)/2 + h_{i,2}(\mathbf{t}_{i,2} \cos \phi_{i,2} + \mathbf{n}_i \sin \phi_{i,2}) \quad (8)$$

$$\mathbf{B}_{i+1} = (\mathbf{C}_i + \mathbf{A}_i)/2 + h_{i,3}(\mathbf{t}_{i,3} \cos \phi_{i,3} + \mathbf{n}_i \sin \phi_{i,3}) \quad (9)$$

$$\mathbf{C}_{i+1} = (\mathbf{A}_i + \mathbf{B}_i)/2 + h_{i,1}(\mathbf{t}_{i,1} \cos \phi_{i,1} + \mathbf{n}_i \sin \phi_{i,1}) \quad (10)$$

- 5) The euclidean distances  $l_{i+1,1...3}$  between the joint points of the new base triangle  $i+1$  are given by:

$$l_{i+1,1} = \|\mathbf{B}_{i+1} - \mathbf{A}_{i+1}\| \quad (11)$$

$$l_{i+1,2} = \|\mathbf{C}_{i+1} - \mathbf{B}_{i+1}\| \quad (12)$$

$$l_{i+1,3} = \|\mathbf{A}_{i+1} - \mathbf{C}_{i+1}\| \quad (13)$$

- 6) Since the angles  $\phi_{i,1...3}$  are not known, (8-10) only form a set of possible solutions for the direct kinematics of a single module. Through the minimization of the error function  $F_{Opt}$ , the positions  $\mathbf{A}_{i+1}$ ,  $\mathbf{B}_{i+1}$  and  $\mathbf{C}_{i+1}$  can be obtained, which are consistent with the given active links' lengths  $L_{i+1,1...3}$  of module  $i+1$ :

$$F_{Opt} = \sum_{n=1}^3 (l_{i+1,n} - L_{i+1,n})^2. \quad (14)$$

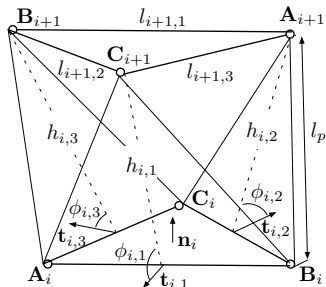


Fig. 7. Variables to describe the direct kinematics of an octahedron VGT.

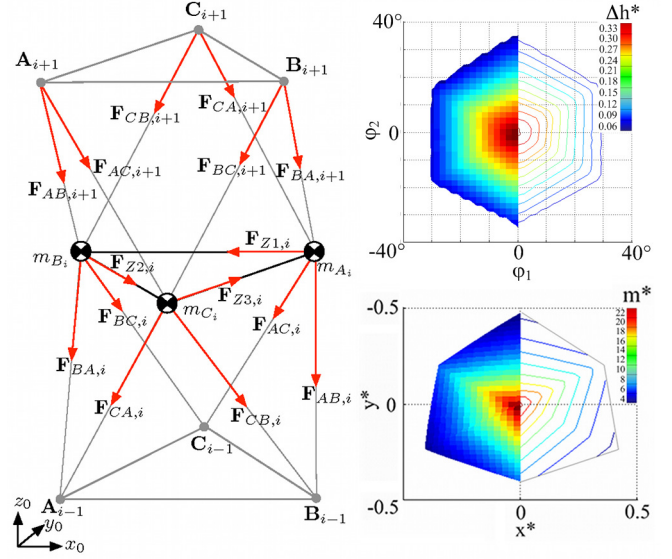


Fig. 8. Left: Static force model for octahedron VGT. Right: Characteristics of one module of the VGT: attainable relative height difference  $\Delta h^* = \Delta h/l_0$  over the module angles  $\phi_1$  and  $\phi_2$  (top) and payload-to-module-weight ratio  $m^*$  over the relative Cartesian displacements  $x^* = x/l_0$  and  $y^* = y/l_0$  with  $l_0$  as the basis side length of the octahedron (bottom).

By applying the presented method to derive the direct kinematic, the workspace of a single module can be calculated, as presented in Fig. 8 (top right).

### B. Computation of link forces and stiffness analysis

For the construction of the VGT and the selection of the actuators, it is necessary to compute the forces in the structure. We present a static force model, which includes the mass of the joints, and the passive and active links, as well as the payload and external forces acting upon the structure.

Due to the fact that the structure is free from bending moments, only compression and pulling forces act within the links. As opposed to the direct kinematic, the forces have to be computed starting out from the top module down to the base module. In order to do this, all masses of the structure elements are transformed into concentrated mass points located in the joints' rotation points. Due to gravitation, these mass points exert a force which is pointing in negative  $z$ -axis direction. Beside the gravitation force, two further forces from the passive links of the overlying module are acting in the joint rotation point, see Fig. 8 (left).

For each module six passive and three active link forces have to be calculated. These nine unknowns can be found by analyzing the following vectorial equations:

$$\begin{aligned} \mathbf{A}_i : \quad & \mathbf{F}_{AC,i} + \mathbf{F}_{AB,i} + \mathbf{F}_{Z1,i} - \mathbf{F}_{Z3,i} + \\ & -\mathbf{F}_{CA,i+1} - \mathbf{F}_{BA,i+1} - m_{A_i} \cdot g \cdot \mathbf{e}_z = 0 \quad (15) \end{aligned}$$

$$\begin{aligned} \mathbf{B}_i : \quad & \mathbf{F}_{BA,i} + \mathbf{F}_{BC,i} + \mathbf{F}_{Z2,i} - \mathbf{F}_{Z1,i} + \\ & -\mathbf{F}_{AB,i+1} - \mathbf{F}_{AC,i+1} - m_{B_i} \cdot g \cdot \mathbf{e}_z = 0 \quad (16) \end{aligned}$$

$$\begin{aligned} \mathbf{C}_i : \quad & \mathbf{F}_{CA,i} + \mathbf{F}_{CB,i} + \mathbf{F}_{Z3,i} - \mathbf{F}_{Z2,i} + \\ & -\mathbf{F}_{AB,i+1} - \mathbf{F}_{AC,i+1} - m_{C_i} \cdot g \cdot \mathbf{e}_z = 0 \quad (17) \end{aligned}$$

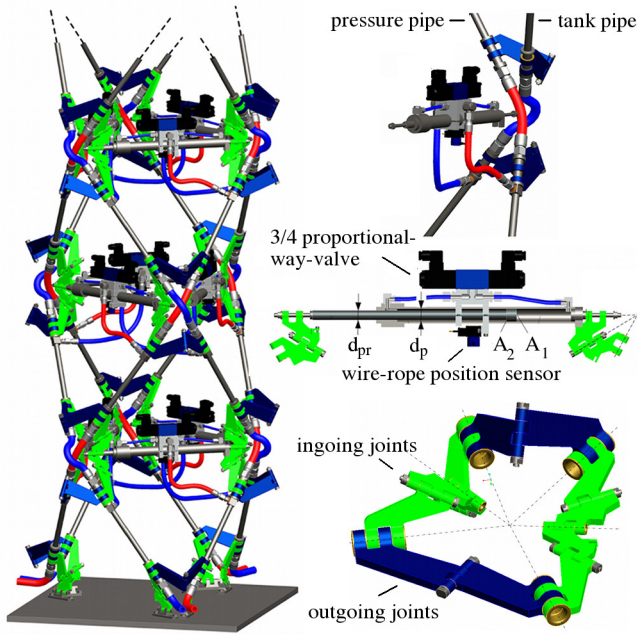


Fig. 9. Left: Assembled robot structure with three modules. Right: routing of hydraulic hoses (top), active link (middle), modified SJM joint (bottom).

A special case is the last module of the structure, where no following modules are present, but gravitation forces are caused by the payload in the tool center point.

From this static force model informations can be derived about the compliance of the components and a module of the VGT and its maximum payload, see Fig. 8 (lower right).

#### IV. COMPOSED STRUCTURE

The designed modules primarily consist of three elements: the passive links, the active links and the multicollated spherical joints. They can be cascaded to form a manipulator as shown in Fig. 9. If more than two modules are combined, the resulting manipulator will have redundant DOFs.

The dimensioning of the hydraulic drives is the last step necessary in the construction of the octahedron VGT module. From the variety of existing hydraulic linear drives, the single rod double acting cylinder is the most feasible for the actuation of the octahedron VGT. In order to achieve a high movability, as well as a large workspace of the kinematic structure, the active link has to realize a high maximum-to-minimum length ratio  $k$ . Beside the high length ratio  $k$  the actuator has to possess a large piston rod area  $A_2 = \pi/4 \cdot (d_p^2 - d_{pr}^2)$  to provide high forces under compression  $F_2 = A_2 \cdot p_{sys}$ . To choose the cylinder for the kinematic structure, an optimum between the length ratio  $k$  and the maximum force  $F_2$ , with respect to the constraints of maximum system pressure  $p_{sys}$  and maximum piston diameter  $d_p$ , has to be found. By using zero lapped 4/3 proportional-way-valves, a good controllability of the actuators and a low energy consumption during holding operations can be achieved.

#### V. CONCLUSION AND FUTURE WORK

In this paper a concept is presented for the design of hydraulically driven modules for a VGT manipulator in octahedron shape. The hydraulic actuation allows high-force actuators, while the separation of power generation and actuators ensures low moved masses. To reduce the necessary hose lengths, the drive fluid is passed through the passive links of the structure which are used as pipes. The structure features special multiple collocated spherical joints based on plates joints, which allow a pinch-free hose connection of the pipes through the joint centers. The danger of collisions between structure elements can be reduced by applying the presented design rules, which lead to the described modified joint design and designated swivel directions for the plate joints. A composition of more than two modules results in a highly maneuverable, kinematically redundant VGT manipulator which is capable of dexterous motion.

Future work will be dedicated to the dynamic characterization of the presented VGT-structure and the setup of an appropriate control architecture.

#### REFERENCES

- [1] G. Chirikjian and J. Burdick, "Hyper-redundant robot mechanisms and their applications," in *IEEE/RSJ International Workshop on Intelligent Robots and Systems '91. 'Intelligence for Mechanical Systems, Proceedings IROS'91.*, vol. 1, Osaka, 1991, pp. 185–190.
- [2] J. Hopkins, B. Spranklin, and S. Gupta, "A survey of snake-inspired robot designs," *Bioinspiration and Biomimetics*, vol. 4, 2009.
- [3] G. Chirikjian and J. Burdick, "A hyper-redundant manipulator," *IEEE Robotics & Automation Magazine*, vol. 1, no. 4, pp. 22–29, 1994.
- [4] M. Mikulas Jr and R. Crawford, "Sequentially deployable maneuverable tetrahedral beam," United States Patent Patent 4 557 097, Dec. 10, 1985, uS Patent 4,557,097.
- [5] K. Miura, "Variable truss concept," The Institute of Space and Astronautical Science, Tech. Rep. 614, 1984.
- [6] P. Hughes, W. Sincarsin, and K. Carroll, "Trussarm - a variable-geometry-truss manipulator," *Journal of Intelligent Material Systems and Structures*, vol. 2, no. 2, pp. 148–160, 1991.
- [7] M. Rhodes and M. Mikulas, "Deployable controllable geometry truss beam," NASA Center: Langley Research Center, Tech. Rep., 1985.
- [8] J. J. Craig, *Introduction to Robotics: Mechanics and Control*. Boston, MA, USA: Addison-Wesley Longman Publishing Co., Inc., 1989.
- [9] G. C. Devol, JR, "Programmed article transfer," Juni 1961.
- [10] V. Scheinman and J. M. McCarthy, *Springer Handbook of Robotics*. Springer Berlin Heidelberg, 2008, ch. Mechanisms and Actuation, pp. 67–87.
- [11] L. Schilling Robotics, *Manual of Schilling Titan 4, Doc. No. 011-8212*, Website., Schilling Robotics, LLC, 2010. [Online]. Available: [www.schilling.com](http://www.schilling.com)
- [12] S. Jacobsen, F. Smith, and D. Backman, "High performance, dextrous telerobotic manipulator with force reflection," in *Intervention/ROV'91 Conf. and Exposition: Subsea Intervention through Education*, 1991, pp. 213–218.
- [13] M. Zhao, T. Gui, G. Chao, Q. Li, and D. Tan, "Development of a redundant robot manipulator based on three dof parallel platforms," in *IEEE International Conference on Robotics and Automation*, 1995.
- [14] J. Hollerbach, I. Hunter, and J. Ballantyne, "A comparative analysis of actuator technologies for robotics," *Robotics Review*, vol. 2, pp. 299–342, 1992.
- [15] R. Isermann, *Mechatronic Systems*. Springer London, 2003, ch. 10 - Actuators, pp. 383–486. [Online]. Available: <http://www.springerlink.de/content/j07t45x12726414x/>
- [16] G. Hamlin and A. Sanderson, "Tetrobot: A modular system for hyper-redundant parallel robotics," in *1995 IEEE International Conference on Robotics and Automation, 1995. Proceedings.*, vol. 1, 1995.

- [17] P. Bosscher and I. Ebert-Uphoff, "A novel mechanism for implementing multiple collocated spherical joints," in *IEEE INTERNATIONAL CONFERENCE ON ROBOTICS AND AUTOMATION*, vol. 1. Cite-seer, 2003, pp. 336–341.